Selective block of adenosine A_{2A} receptors prevents ischemic-like effects induced by oxygen and glucose deprivation in rat medium spiny neurons

Elisabetta Coppi[1], Alasdair J Gibb[2]

[1]Dept. of Neuroscience, Psychology, Drug Research and Child Health, University of Florence, Florence, Italy; [2]Department of Neuroscience, Physiology and Pharmacology, University College London, Gower Street, London WC1E 6BT, UK.

Corresponding author: Elisabetta Coppi (elisabetta.coppi@unifi.it) and Alasdair J Gibb (a.gibb@ucl.ac.uk)

Abstract

Background and Purpose. Ischemia is known to cause massive neuronal depolarization, termed anoxic depolarization (AD), due to energy failure and loss of membrane ion gradients. The neuromodulator adenosine accumulates extracellularly during ischemia and activates four metabotropic receptors: A_1, A_{2A}, A_{2B} and A_3. Striatal medium spiny neurons (MSNs) express high levels of A_{2A} receptors (A_{2A}Rs) and are particularly vulnerable to ischemic insults. It is known that A_{2A}R blockade reduces acute striatal post-ischemic damage but the cellular mechanisms involved are still unknown.

Experimental Approach. We performed patch-clamp recordings from MSNs in rat striatal slices subjected to oxygen and glucose deprivation (OGD) in order to investigate the effects of A_{2A}R ligands or ion channel blockers on AD and OGD-induced ionic imbalance, measured as a positive shift in E_{rev} of ramp currents.

Key Results. Our data indicate that the A_{2A}R antagonist SCH58261 (10μM) significantly attenuated ionic imbalance and AD appearance in MSNs exposed to OGD. The K^+ channel blocker Ba^{2+} (2mM) or the Na^+ channel blocker tetrodotoxin (1μM) exacerbated and attenuated, respectively, OGD-induced changes.

Spontaneous excitatory post-synaptic current (sEPSC) analysis in MSNs revealed that the A_{2A}R agonist CGS21680 (1μM) prevented OGD-induced decrease of sEPSCs within the first 5 min of the insult, an effect shared by the K^+ channel blocker Ba^{2+}, thus indicating facilitated glutamate release.

Conclusion and Implications. We conclude that adenosine, released during striatal OGD, activates A_{2A}Rs that may exacerbate OGD-induced damage through K^+ channel inhibition. Our results could help to develop A_{2A}R-selective therapeutic tools for the treatment of brain ischemia.

This article has been accepted for publication and undergone full peer review but has not been through the copyediting, typesetting, pagination and proofreading process which may lead to differences between this version and the Version of Record. Please cite this article as doi: 10.1111/bph.15922

- **What is already known**

Adenosine A1, A2 and A3 receptor subtypes affect neuroprotective signalling during ischaemic brain damage.

- **What this study adds**

This study improves understanding of A2A receptor mechanisms during anoxic depolarisation in rat striatal neurons.

- **Clinical significance**

Our results suggest $A_{2A}R$ blockade may be protective by delaying and reducing the anoxic depolarisation.

1. Introduction

Stroke is a major cause of brain damage and permanent disability worldwide but current treatments have limited therapeutic success. Much of post-ischemia neuronal death is triggered by exaggerated glutamate release (Choi & Rothman, 1990) resulting from a fall in cytoplasmic ATP concentration which causes a loss of plasma membrane Na^+/K^+-ATPase activity and transmembrane ion gradients with consequent neuronal and glial depolarization. This condition induces an abrupt increase in extracellular K^+ concentration ($[K^+]_o$) (Erecinska & Silver, 1994; Hansen, 1985) causing a massive release of neurotransmitters in the injured brain area and in particular an exaggerated glutamate release, partly due to vesicular release and mostly due to the reversal of glutamate transporters (Madl & Burgesser, 1993; Rossi et al., 2000; Szatkowski et al., 1990). Once released, extracellular glutamate activates ionotropic alpha-amino-3-hydroxy-5-methyl-4-isoxazolepropionic acid (AMPA) receptors (AMPARs) as well as N-methyl-D-aspartate (NMDA) receptors (NMDARs) that contribute to exaggerated depolarization and Ca^{2+} influx ultimately leading to anoxic depolarization (AD) and neuronal death.

Whether an AD occurs during transient ischemia and its time of occurrence are key factors influencing neurological deficits and the extent of the resulting brain damage. Adenosine signalling is a ubiquitous mechanism by which neurons and glial cells communicate with each other. Extracellular adenosine levels in the brain are generally in the nM range but, under pathological conditions such as brain ischemia, adenosine is released in huge amounts (Pedata et al., 2016) and activates all subtypes of adenosine receptors, namely A_1, A_{2A}, A_{2B}, and A_3 receptor subtypes (A_1R, $A_{2A}R$, $A_{2B}R$ and A_3R) (Fredholm et al., 2011).

The increase in extracellular adenosine during hypoxia/ischemia is thought to play a neuroprotective role through the activation of A_1Rs, which are highly expressed in the brain (Dunwiddie & Diao, 1994). The other G_i-coupled adenosine receptor subtype, the A_3R, proved to exert either protective (Pugliese et al., 2007) or detrimental effects (Pugliese et al., 2006; von Lubitz et al., 1999) during brain ischemia, depending on the experimental model used or timing of A_3R ligand application. Interestingly, selective block of G_s-coupled A_{2B}Rs during and *in vitro* ischemic-like insult, i.e. oxygen and glucose deprivation (OGD), is protective in acute hippocampal slices because it causes a delay in AD appearance and a reduction in CA1 astrogliosis, cytochrome C release and neuronal loss (Fusco et al., 2018), effects possibly mediated by inhibition of glutamate release (Fusco et al., 2019; Goncalves et al., 2015). On the other hand, in *in vivo* models of transient middle cerebral artery occlusion (tMCAo), A_{2B}Rs agonists reduce brain damage, neuroinflammation and neurological deficit in rats (Dettori et al., 2021) possibly by inhibiting tissue plasminogen activator (tPA) and protecting cerebrovascular integrity (Li et al., 2017).

The other G_s-coupled adenosine receptor, the $A_{2A}R$, is known to be a crucial mediator of ischemic injury in the hippocampus (Maraula et al., 2013) and striatum (Pedata et al., 2016). Its block by the $A_{2A}R$ antagonist SCH58261 during acute ischemic injury, or during the post-ischemic phase (i.e. within 24 h after tMCAo), proved protective by reducing neurotransmitter outflow, histological damage and neurological impairment (Melani et al., 2003). Furthermore, SCH58261 also prevented oxidative stress and neuronal injury after acute hypoxic insults in the striatum of new-born piglets (Ortega-Gutierrez et al., 2020). However, when the $A_{2A}R$ antagonist was administered over 7 days after the insult, the protection from neurological deficit was lost (Melani et al., 2015). Indeed, the administration of the selective $A_{2A}R$ agonist CGS28561 at later phases after the insult (i.e. 7 days after tMCAo) protected the post-ischemic brain tissue by reducing peripheral immune cell infiltration (Melani et al., 2014), in line with the well known anti-inflammatory role of $A_{2A}Rs$ in peripheral cells (Antonioli et al., 2013). Taken together, the above data demonstrate that ischemia-induced early excitotoxicity can be relieved by $A_{2A}R$ antagonists whereas, at later times after the insult, secondary neuroinflammation requires $A_{2A}R$ agonist-mediated neuroprotection.
Of note, no data are reported to date about the effect of $A_{2A}R$ ligands in MSNs during an OGD insult. In the present study, we performed patch-clamp recordings in MSNs from acute striatal slices to elucidate the mechanisms by which an ischemic-like insult, obtained *in vitro* by OGD, causes functional impairment in these cells and to study the involvement of $A_{2A}Rs$ in these events.

2. Methods

2.1 Solutions. Slicing solution was (in mM): sucrose, 206; KCl, 2.5; $CaCl_2$ 1, $MgCl_2$ 4; NaH_2PO_4 1.25, $NaHCO_3$ 25, kynurenic acid 0.1, glucose 25, pH 7.4 when saturated with 95% O_2 and 5% CO_2. Recording solution was (in mM): NaCl 125, KCl 2.5, $CaCl_2$ 1, $MgCl_2$ 1, NaH_2PO_4 1.25, $NaHCO_3$ 25, glucose 25, pH 7.4 when saturated with 95% O_2 and 5% CO_2. Slicing and recording solutions were gassed continuously with a mixture of O_2 (95%) and CO_2 (5%). OGD solution was obtained by replacing glucose with equimolar sucrose in the recording solution and by bubbling with 95% N_2 and 5% CO_2. Pipette solution was (in mM): K-gluconate 130, NaCl 4.8, $MgCl_2$ 2, $CaCl_2$ 1, EGTA 0.2, HEPES 10, adjusted to pH 7.4, with KOH. Pipette solution was stored at -20°C in 1 ml aliquots. Before starting the experiment, Na_2ATP 2 mM and NaGTP 0.3 mM were added daily to each aliquot of pipette solution stored on ice during use.

2.2 Brain slice preparation. Striatal slices were prepared as described elsewhere (Coppi et al., 2012). Briefly, Sprague–Dawley rats (aged 28 days postnatal: P28) were deeply anaesthetized with isofluorane and decapitated in accordance with the UK Animals (Scientific Procedures) Act 1986 and Local Ethical Committee approval. Animal studies were in compliance with the ARRIVE guidelines (Percie du Sert et al., 2020) and with the recommendations made by the British Journal of Pharmacology (Lilley et al., 2020). Every effort was made to minimize animal suffering and the number of animals used. The brain was removed from the skull and submerged in ice-cold oxygenated slicing solution. Coronal brain slices (300 µm thick) were prepared using a vibrating microslicer (Leica VT1000, Germany) and incubated at room temperature (20–24°C) in oxygenated recording solution for 1–6 h before use. A single slice was then transferred into a 0.3 ml incubation chamber continuously superfused (2 ml/min) with oxygenated recording solution by a six-way, gravity-fed system. When indicated, $A_{2A}R$ ligands or ion channel blockers were added to the recording solution and perfused for at least 10 min before OGD. In particular, the Na^+ channel blocker tetrodotoxin (TTX, 1 µM), the K^+ channel blocker Ba^{2+} (2 mM), the $A_{2A}R$ agonist CGS21680 (1 µM) or the $A_{2A}R$ antagonist SCH58261

(10 μM) were used in the present research. CGS21680 and SCH58261 concentrations were chosen (using the Gaddum equation) to give receptor occupancy ~ 90% in control and to reduce adenosine receptor occupancy during OGD to less than 10% in presence of SCH58216 assuming extracellular adenosine concentrations of 100 nM and 20 μM in control and during OGD respectively (Pedata et al., 2016).

2.3 Data and statistical analysis. The present research was performed on n=21 control cells recorded from 21 slices prepared from 16 animals, n=12 cells recorded from 12 SCH58261-treated slices prepared from 5 animals, n=11 cells recorded from 11 CGS21680-treated slices prepared from 5 animals, n=10 cells recorded from 10 Ba^{2+}-treated slices prepared from 5 animals and n=10 cells recorded from 10 TTX-treated slices prepared from 5 animals. Each slice recording was made independently and recordings were grouped per animal for statistical analysis. Sample size estimation and power analysis was performed using G*Power (Version 3.1.9.6 – available from https://gpower.software.informer.com/3.1/). Randomisation and blinding of slice treatments was not done due to the nature of the primary experimental manipulation (e.g. change to solution with oxygen and glucose deprivation). All statistical comparisons between groups were made for n = 5 or more rats per groups as detailed above. Shapiro-Wilk normality test was performed to check data distribution. As most of the data tested negative (i.e. not normally distributed), statistical analysis was made uniformly with non-parametric tests, unless otherwise stated. Averaged data are reported as median ± 95% confidence interval (CI). Wilcoxon or Dunn's multiple comparison non-parametric tests were performed, as appropriate, in order to determine statistical significance (P<0.05). Data were analysed using "GraphPad Prism" (San Diego, CA, USA) software. The data and statistical analysis comply with the recommendations on experimental design and analysis in pharmacology (Curtis et al., 2018). Technical replicates were used to ensure the reliability of single values. No exclusion criteria were applied to any of the experimental data.

2.4 Whole-cell recordings. Patch pipettes were pulled from thick-walled borosilicate glass capillaries (GC150F-7.5, Harvard Apparatus, Holliston, MA) to final resistance of 4–7 MΩ. Membrane voltages given in the results are corrected for a calculated liquid junction potential of -8 mV. To reduce the voltage error due to the series resistance (Rs), 75-80% of the Rs was compensated before starting recordings. The cell bodies of individual neurons in brain slices were visualized under Nomarski differential interference contrast optics. Medium spiny neurons (MSNs) comprise about 90% of striatal neurons (Rymar et al., 2004) and are characterized by a resting membrane potential (RMP) around -80 mV, a small cell diameter (~20 μm) and a membrane resistance (R_m) of about 300 MΩ (Cao et al., 2018). The present research was performed on n=64 cells identified as striatal MSNs on the basis of their location, size, morphology and electrophysiological properties: cells had a mean RMP of -80.2 ± 0.7 mV, a cell capacitance (C_m) of 22.3 ± 1.6 pF and a R_m of 185.6 ± 17.6 MΩ.

2.5 Voltage-clamp experiments. Whole-cell currents were recorded as previously described (Coppi et al., 2012). Briefly, recordings were made using an Axopatch 200B amplifier, filtered at 1 kHz (8-pole Bessel) and digitized at 10 kHz using an analogue-to-digital converter (CED micro 1401, Cambridge Electronic Design, UK). Cells were voltage clamped at -60 mV and the holding current (I_h) continuously monitored throughout the experiment. Four successive voltage ramps (from -118 to -63 mV, 1 s duration, 2 s inter-episode interval) were applied to the cell every 1 min and recorded using the program WinEDR (available from Strathclyde Electrophysiology Software, Glasgow, UK, at http:// spider.science.strath.ac.uk/PhysPharm/showPage.php?pageName_software_ses). All ramp traces shown in the figures are the average of four consecutive ramp episodes collected at 2 s

inter-episode interval. Spontaneous excitatory post-synaptic currents (sEPSCs) in MSNs were recorded at -60 mV throughout the experiment and detected by using the 'template' function in the program WinEDR. When TTX was present in the bath solution, spontaneous AP-independent miniature excitatory post-synaptic currents (mEPSCs) were recorded by the same method. Traces were digitally filtered (low pass 540 Hz) for analysis.

2.6 Oxygen and glucose deprivation (OGD). Experiments were performed as described (Fusco et al., 2018). Briefly, after a stable baseline (less than ~10% variation) of I_h and ramp currents was acquired for at least 5 min, OGD was applied by switching to a glucose-free and oxygen-deprived (i.e. continuously bubbled with a mixture of 95% N_2 and 5% CO_2) recording solution. OGD was continued until 1 min after the appearance of AD peak, measured by increased I_h. After the AD was completed (i.e. when I_h reached a negative steady-state level), slices were reperfused with standard, glucose-containing and oxygenated, recording solution. Changes in membrane ionic balance during OGD were monitored by quantifying the "zero current potential" (E_{rev}) of ramp currents before and during the insult. E_{rev} was measured by interpolating each averaged ramp trace with a polynomial equation and solving for "y=0". Changes in R_m during OGD were quantified by isolating averaged ramp traces between -90 and -70 mV and fitting a straight line to those data points. The value of the slope corresponds to the inverse of R_m.
All pre-OGD values were measured 2 min before OGD start. AD latency was measured as the time between OGD start and the time at which I_h increased by more than 20% of pre-OGD level. The "AD peak time" was measured as the time between OGD start and the time at which I_h reached its maximal negative peak. The latency between I_h change > 20% and AD peak was measured as the difference between AD latency and "AD peak time" AD peak amplitude was measured as the difference between pre-OGD I_h value and the maximum negative peak recorded during OGD. The latency for R_m decrease during OGD was measured as the time between OGD start and the time at which R_m changed more than 20% from pre-OGD value. Changes in E_{rev} during OGD were measured by subtracting the pre-OGD value from that measured between 15 and 18 min OGD. Assuming this is dominated by changes in $[K^+]_o$, the predicted $[K^+]_o$ before or during OGD, E_{rev} was extrapolated from Nernst's equation:
$E_{rev} = RT/zF \ln([K^+]_o/[K^+]_i)$
where *z* is the ion charge, *R* is the gas constant, *F* is the Faraday's constant and *T* is the temperature in °K, by substituting respective E_{rev} values measured as the "zero current potential" of 4 averaged voltage ramps elicited 1 min before OGD or during AD peak. The latency to E_{rev} inflection point was measured as the time between OGD start and the time of inflection point (the time at which the straight line interpolating data points in the pre-OGD phase crosses the straight line interpolating data points during I_h increase > 20% until the end of OGD).

2.7 Drugs and chemicals. NaCl, NaOH, NaH_2PO_4, NaHCO3, KCl, $BaCl_2$, $CaCl_2$, $MgCl_2$, sucrose, CsCl, NMDG, and glucose were purchased from BDH Laboratory Supplies (Poole, England). HEPES, EGTA, ATP, GTP, were purchased from Sigma (St. Louis, MO). Tetrodotoxin (TTX) was purchased from Ascent Scientific (Bristol, UK) or Alomone Labs (Jerusalem, Israel). The concentrations of the $A_{2A}R$ agonist CGS21680 (1 µM) and antagonist SCH58261 (10 µM) were chosen on the basis of ligand-binding studies from Cunha et al., (Cunha et al., 1999) and from Zocchi et al., (Zocchi et al., 1996), respectively.

2.8 Nomenclature of targets and ligands.
Key protein targets and ligands in this article are hyperlinked to corresponding entries in the IUPHAR/BPS Guide to PHARMACOLOGY http://www.guidetopharmacology.org and are

permanently archived in the Concise Guide to PHARMACOLOGY 2021/22 (Alexander et al., 2021).

3. Results

3.1. OGD-induced appearance of anoxic depolarization in rat striatal MSNs is delayed by the A2AR antagonist SCH58261.

We performed patch-clamp recordings from rat striatal MSNs in order to detect whether the electrophysiological changes induced by an OGD insult in these cells are modified by $A_{2A}R$ selective block. The amplitude of I_h was measured before and during OGD by clamping MSNs to -60 mV. Furthermore, in order to monitor estimated changes in $[K^+]_o$ and/or R_m, we applied voltage ramp protocols before, during and after the insult (Fig. 1a, lower inset).

As shown in Figure 1A, a prolonged OGD insult caused an abrupt increase in I_h at -60 mV. This event is commonly called anoxic depolarization (AD) and is primarily due to a loss of electrochemical gradients and consequent neuronal depolarization, exacerbated by extracellular glutamate accumulation (Allen et al., 2004; Rossi et al., 2000). Immediately before AD, a series of events are observed which can be recapitulated as follow: 1) a "slow phase" of electrophysiological changes consisting in I_h increase (see Fig. 1a between "a" and "b") and a gradual positive shift in the "0 current" potential of the voltage ramp likely resulting from loss of K^+ from neurons in the slice and opening of neurotransmitter-gated ion channels (Fig. 1b: see differences between trace "a" and trace "b"); 2) sporadic downward deflections observed during the voltage ramp at potentials around -65/-55 (Fig. 1b trace b) representing action potentials (APs) detected as inward action currents in voltage-clamp mode; 3) a massive increase in inward ramp currents simultaneous to a marked shift in the ramp "zero current potential" (Fig. 1b trace c) and, lastly, 5) a drop in I_h at -60 mV (arrowhead in Fig. 1a) corresponding to the AD. Concerning point 2, repetitive AP firing was observed in 67 % of MSNs (10 out of 15 cells recorded). These currents were never observed when OGD was performed in the presence of TTX (see below). The increase in ramp currents (point 3) is consistent with a reduction in R_m during OGD whereas the positive shift in E_{rev} is mainly indicative of changes in the reversal potential for K^+ ions due to extracellular K^+ accumulation during anoxia (Hansen, 1985). Figure 1c shows the time course of changes in I_h, R_m and E_{rev} in a representative MSN subjected to OGD. These changes were statistically significant when measured in 15 control OGD neurons (Fig. 1d) and are in line with previous results in the literature from hippocampal CA1 neurons (Rossi et al., 2000). Of note, the calculated $[K^+]_o$ at AD peak, measured by extrapolation from respective E_{rev} values by Nernst equation, was 30.0 ± 1.2 mM, consistent with previous data from the hippocampus reported in the literature (Hansen, 1985).

Furthermore, the latency to R_m decrease (>20% change from pre-OGD level) measured in 15 control OGD experiments was 7.6 min (454 s: central bar in Fig. 1e), a value significantly smaller than that observed for I_h increase, i.e. 10 min (604 s: left bar in Fig. 1e). In contrast, the latency to E_{rev} shift (inflection point in E_{rev}) was 8.1 min (488.8 s: right bar in Fig. 1e), a value not significantly different from the latency to R_m nor I_h changes.

As mentioned above (point 2), in some cases (10 out of 15 MSNs recorded, 67 %), a spontaneous burst of APs (arrow in Fig. 2a and expanded time scales in Fig. 2b,c) was observed during AD. This phenomenon has been previously described by others during hypoxia (Guatteo et al., 1998; Karunasinghe & Lipski, 2013). When observed, the latency to spontaneous AP burst was 12.6 min (692.5 s) from OGD start (Fig. 2d, left panel), lasted for 15.7 s (Fig. 2b, central panel) and had an averaged frequency of 7.2 Hz (Fig. 2d right panel).

We then investigated the effect of selective $A_{2A}R$ ligands on the OGD-induced changes in electrophysiological parameters described above. When OGD was performed in the presence

of the $A_{2A}R$ antagonist SCH58261 (10 µM), AD appearance was significantly delayed (Fig. 3a) and E_{rev} depolarization was significantly smaller (Fig. 3c). Of note, only 3 out of 5 (60 %) experiments performed in SCH58261 presented a spontaneous AP burst during AD. On the other hand, when OGD was performed in the presence of the $A_{2A}R$ agonist CGS21680 (1 µM), neither AD latency, amplitude nor E_{rev} changes were different from control (Fig. 3a-c). Of note, 4 out of 5 (80 %) experiments performed in CGS21680 presented spontaneous AP bursts during AD. However, the latency of this phenomenon was similar to what was observed in control slices (Fig. 3d).

We then tested the involvement of voltage-gated K^+ or Na^+ channels in OGD-induced electrophysiological changes by performing OGD in the presence of K^+ or Na^+ channel blockers: Ba^{2+} (2 mM) or TTX (1 µM), respectively. As shown in Figure 3a, neither of these compounds affected AD latency. However, AD amplitude and E_{rev} changes during OGD were significantly attenuated in the presence of TTX (Fig. 3b,c) and, in addition, the latency between AD appearance (>20% increase in I_h) and AD maximum I_h (lowest value of I_h reached) was significantly increased (Fig. 3e), indicating that TTX decelerates the rate at which AD deflection occurs before the I_h drop. As expected, none of the MSNs investigated presented spontaneous bursting activity in the presence of TTX (Fig. 3c), thus confirming that this phenomenon depends on voltage-gated Na^+ channel-dependent AP firing.

As summarized in Figure 3f, the selective block of $A_{2A}Rs$ delayed AD appearance and reduced its amplitude, whereas their activation exacerbated AD. Similarly, E_{rev} depolarization was significantly decreased by the $A_{2A}R$ blocker SCH58261 and enhanced by the $A_{2A}R$ agonist CGS21680. Furthermore, K^+ channel block exacerbated, whereas Na^+ channel block mitigated, OGD-induced changes in I_h and E_{rev}.

The effects of the K^+ channel blocker Ba^{2+} on OGD-induced changes are reported in detail in Figure 4. During the pre-OGD phase, Ba^{2+} (2 mM) caused a modest, but significant, increase in the I_h at -60 mV indicating, as expected, neuronal depolarization upon K^+ channel block (Fig. 4a). Indeed, I_h was usually measured as a positive value in MSNs in our experimental conditions, consistent with the fact that the resting membrane potential (RMP) of these cells is about -70 mV or below (Cao et al., 2018). After 5 min of Ba^{2+} application, I_h significantly decreased (Fig. 4c and 4d upper panels: from 62.7 ± 8.9 pA in control to -14.2 ± 9.3 pA in 2 mM Ba^{2+}, n=5). Furthermore, a significant increase in R_m (Fig. 4c and 4d middle panels) and a positive shift in E_{rev} (Fig. 4c and 4d lower panels: calculated $[K^+]_o$ in Ba^{2+} during the pre-AD phase was 15.2 ± 1.1 mM) were measured in the pre-OGD period, in line with K^+ channel block. Then, when OGD was carried out in the presence of extracellular Ba^{2+}, I_h change was similar to the control group: a slow increase in I_h (Fig. 4c,d; lower panels) preceded I_h drop corresponding to the AD. Of note, E_{rev} increase during OGD was markedly exacerbated in Ba^{2+}-treated slices, consistent with a more pronounced accumulation of extracellular K^+ in these conditions. In fact, the estimated $[K^+]_o$ at AD peak when extracellular Ba^{2+} is present was 118.7 ± 3.4 mM, indicating an exacerbation of extracellular K^+ overload during OGD.

Finally, it is note-worthy that AD appearance during OGD is known to be temperature sensitive (Rosen & Morris, 1994). So, we continuously monitored the temperature of the recording chamber before, during and after OGD. Figure S1 shows that no significant differences were found in the bath temperature during OGD among different experimental groups (Fig. S1).

3.2. OGD induced inhibition of spontaneous synaptic current frequency in MSNs is prevented by the $A_{2A}R$ agonist CGS58261 and by K+ channel block.

In order to gain insight into the mechanisms by which $A_{2A}Rs$ contribute to OGD-induced neuronal damage, we measured the frequency and amplitude of spontaneous excitatory post-synaptic currents (sEPSCs) as an index of overall striatal synaptic excitability before or during the ischemic-like insults carried out in the presence of drugs or in Ba^{2+} or in control conditions.

As shown in Figure 5, following initiation of OGD there was a significant decrease in sEPSC frequency (Fig. 5a and b, blue symbols) in the period between 3-5 min of OGD, indicating a decreased probability of glutamate release as the insult starts, before proceeding to a complete loss of synaptic transmission likely due to energy depletion. No changes were measured in sEPSC amplitude (Fig. 5c, left panel). When OGD was carried out in the presence of the $A_{2A}R$ antagonist SCH58261 (10 µM), the decrease in sEPSC frequency was preserved (Fig. 5a and b, yellow symbols) but, at variance, it was completely prevented by the selective $A_{2A}R$ agonist CGS21680 (1 µM: Fig. 5a and b, orange symbols). This result indicates that selective $A_{2A}R$ activation counteracts OGD-induced inhibition of neurotransmitter release. A similar effect was observed when OGD was performed in the presence of extracellular Ba^{2+} (2 mM): OGD-induced decrease in sEPSC frequency was absent during K^+ channel block (Fig. 5a and b, purple symbols). Of note, no significant changes were observed in the sEPSC amplitude before or during OGD in any of the experimental group investigated (Fig. 5c), suggesting no differences in the expression level of AMPARs on the post-synaptic membrane.
Finally, when TTX (1 µM) was added to the extracellular solution, spontaneous mEPSCs (miniature excitatory post-synaptic currents) were observed. Unlike sEPSCs which are AP-dependent synaptic events, mEPSCs give a measure of spontaneous AP-independent quantal neurotransmitter release (Wu et al., 2007). Our data demonstrate that OGD did not influence the frequency nor the amplitude of mEPSCs in rat MSNs suggesting no change in the post-synaptic response to glutamate release (Fig. 5a-c, green symbols).

4. Discussion

The present work demonstrates, for the first time, that the selective block of $A_{2A}Rs$ in rat striatal slices protects MSNs from OGD-mediated insults by delaying the appearance of AD.
Brain ischemia is known to produce severe neurological impairments associated with neuroinflammation and neurodegeneration. Much of ischemia-induced neuronal death is triggered by exaggerated glutamate release (Choi & Rothman, 1990; Tambasco et al., 2018; Rossi et al., 2000). Extracellular K^+ increase and massive neuronal depolarization are among the main triggers of glutamate-mediated excitotoxicity and significantly contribute to metabolic imbalance and AD appearance (Blank & Kirshner, 1977). However, the failure of glutamate receptor antagonists to protect from stroke-induced neuronal death (Ikonomidou & Turski, 2002) in the clinic has stimulated research towards new approaches for the treatment of brain ischemia, including those based on avoiding uncontrolled neuronal depolarization upon energy failure. Encouraging results came from studies aimed to promote K^+ channel opening after stroke. Early treatment with K^+ channel openers, in particular those targeting ATP-sensitive K^+ channels, blocked the expression of a number of ischemia-induced immediate early genes and protected neuronal cells from degeneration (Heurteaux et al., 1993). Furthermore, the prototype M-channel ‘‘opener’’ retigabine reduced the cascade of deleterious events following traumatic brain injury, including hyperexcitability, ischemia/hypoxia-related metabolic stress and cell death (Vigil et al., 2020). These studies suggest that early reduction of neuronal excitability and energy demand via K^+ current enhancement may provide an efficacious therapeutic intervention against post-ischemic brain damage.
Adenosine is an important neuromodulator in the CNS and is massively released during hypoxic/ischemic conditions (Pedata et al., 2016). Interestingly, $A_{2A}Rs$, which are highly expressed in the striatum, specifically on dopamine D2 receptor-containing MSNs (Le Moine et al., 1997), are associated with K^+ channel inhibition in different cell types and, *vice versa*, $A_{2A}R$ antagonists induce K^+ channel opening in several experimental models (Saegusa et al., 2004; Duffy et al., 2007; Coppi et al., 2013). It could be argued that the mechanism by which $A_{2A}R$ block in MSNs during OGD delays AD appearance is the enhancement of K^+ currents

and consequent reduction of cell excitability. This hypothesis is in line with the fact that, when OGD is carried out in the presence of the $A_{2A}R$ antagonist SCH58261, E_{rev} shift is significantly reduced suggesting a less severe extracellular $[K^+]$ overload, and AD latency is delayed, indicating that striatal MSNs can endure a longer OGD period before undergoing irreversible energy failure. In contrast, the selective $A_{2A}R$ agonist CGS21680, as well as the K^+ channel blocker Ba^{2+}, enhanced the E_{rev} shift and AD amplitude. Furthermore, while OGD decreased sEPSC frequency in the first phases of the insult, either $A_{2A}R$ agonism or Ba^{2+} oppose this "protective" mechanism in the injured brain slice to control neuronal over-excitation during energy failure, thus enhancing glutamate release probability during the first minutes of OGD as compared to control slices.

Concerning the nature of the inward current/s underlying the AD, data in the literature demonstrated that I_h increase during prolonged OGD is mostly due to AMPAR plus NMDAR activation (Rossi et al., 2000), with a contribution of $GABA_A$-mediated Cl^- currents, depending on the experimental conditions used (Allen et al., 2004). As we used a low Cl^-–based pipette solution, $GABA_A$ receptor activation in our recording conditions would result in outward currents, unlikely to contribute to overall AD current. Among the two glutamate-dependent components of the AD signal, the NMDAR- and the AMPAR-dependent, the major part is likely to be due to the NMDAR subtype because of: 1) the removal of Mg^{2+} block upon OGD-induced depolarization; 2) higher affinity of NMDARs for glutamate; and 3) the lack of receptor desensitization upon prolonged agonist exposure, as in the case of AMPARs. Thus, most of the AD current is likely carried by Na^+ and Ca^{2+} ion entry which triggers a variety of deleterious events ultimately leading to neuronal death. This is in line with previous data showing a close temporal correlation between ionic changes in the ischemic hippocampus and glutamate outflow (Rossi et al., 2000). Noticeably, inward deflections in the direct current potential, used to detect *in vivo* AD, go along with extracellular striatal glutamate increase in the dialysate of rats subjected to brief (3-5 min), repeated bilateral ischemic episodes (Ueda et al., 1992).

In the present study, we also get insight into the mechanisms by which $A_{2A}Rs$ modulate functional impairment during an ischemic-like insult *in vitro* by measuring a number of electrophysiological parameters that are affected by OGD. We simultaneously recorded I_h, R_m and E_{rev} in order to detect the timeline of electrical changes induced by the insult. We found that, during OGD, R_m decreased and E_{rev} depolarized. In particular Rm decrease, consistent with an increase in membrane leakage, preceded the I_h increase induced by OGD. We conclude that, in striatal MSNs, OGD-induced energy failure and the consequent loss of ion gradients across the cell membrane leads to overall channel opening (R_m decrease) and $[K^+]_o$ accumulation (E_{rev} depolarization) leading to AD and irreversible neuronal damage.

In some cells (67%), AD was preceded by a spontaneous burst of APs. This phenomenon has been previously described by others and is related to OGD-induced depolarization leading to the activation of voltage-dependent Na^+ channels (Guatteo et al., 1998; Jarvis et al., 2001), but the reason why some cells fire spontaneous APs and some others do not, is not clear. We hypothesize that, if membrane depolarization is slow enough (for example due to the fact that the recorded cell is near the surface of the slice so that fluid perfusion is more effective in removing excess extracellular K^+ nearby the recorded cell) to activate Na^+ channels before causing their inactivation, some APs may arise before the neurons become electrically unexcitable. On the other hand, if cells recorded are deeper inside the brain slice, $[K^+]_o$ may rise more quickly thus leading directly to Na^+ channel inactivation before any significant activity starts.

We then investigated the influence of different voltage-gated ion channels on AD appearance by using a pharmacological approach. When OGD was carried out in the presence of the Na^+ channel blocker TTX, AD latency (the time at which I_h changes more than 20%) was

unchanged in comparison to control OGD slices, but the time at which AD reached its maximal negative peak was significantly delayed and AD amplitude was reduced, indicating a slower AD deflection in the presence of TTX. Hence, our data demonstrate that voltage-dependent Na^+ channels are not involved in initial changes in membrane permeability leading to AD initiation but, however, they accelerate and exacerbate the achievement of maximal AD amplitude.

It is noteworthy that, when OGD was carried out in the presence of extracellular Ba^{2+}, ramp currents still increased in the pre-AD phase, demonstrating that, at least in these conditions, OGD not only activates K^+ currents but, in addition, other conductances just before the I_h drops. We hypothesize that a possible candidate for this increased conductance during OGD is Cl^-. Indeed, MSNs are GABAergic and the large ramp-current increase observed in the pre-AD phase when in extracellular Ba^{2+} is likely due to huge GABA release during early excitotoxicity producing the activation of many $GABA_A$ receptors. A significant contribution of GABA to the AD current has been demonstrated before (Allen et al., 2004).

We also measured sEPSCs before and during OGD in different experimental conditions, in order to gain insight into the presynaptic and postsynaptic effects of OGD and/or A_{2A}Rs during the pre-AD phase. We found that OGD insults, carried out in control conditions, significantly reduced sEPSC frequency, indicating a reduction of neurotransmitter release during the first phases of OGD (Arcangeli et al., 2013). These data are consistent with previous results demonstrating that A_1R agonists inhibit glutamate release (Oliet & Poulain, 1999). Indeed, during hypoxic/ischemic conditions, the huge release of endogenous adenosine leads to robust A_1R activation which, in turn, reduces vesicular neurotransmitter release (Pedata et al., 2016). On the other hand, when we performed OGD in the presence of the A_{2A}R agonist CGS21680, the reduction in sEPSC frequency observed in the first minutes of the insult was prevented. This is in line with previous data showing that A_{2A}R activation facilitates neurotransmitter release either during normoxic (Lopes et al., 2002) or ischemic (Melani et al., 2003; Gui et al., 2009) conditions. In particular, the work by Gui and collaborators demonstrated that A_{2A}R-KO mice presented a reduced glutamate outflow in the striatum after transient MCAo which correlates with reduced neurological deficit and cerebral infarct volume, thus suggesting that the protection of A_{2A}R inhibition is associated with the suppression of glutamate-dependent toxicity. Of note, Ba^{2+} also prevented the OGD-induced reduction in sEPSC frequency, in line with the fact that K^+ channel block induces neuronal depolarization and thus facilitates neurotransmitter release. Finally, OGD did not altered sEPSC amplitude in any of the experimental conditions tested, indicating no changes in the expression of postsynaptic AMPARs nor NMDARs.

In conclusion, we demonstrated here that A_{2A}R blockade during OGD protects striatal MSNs by reducing AD amplitude and delaying AD appearance possibly by enhancing K^+ currents. Our data could help to develop A_{2A}R antagonists as new pharmacological tools for the treatment of acute ischemic damage during brain ischemia.

Acknowledgements.

The present research was supported by the University of Florence (58514_Internazionalizzazione and Fondi Ateneo Ricerca); by FISM (Fondazione Italiana Sclerosi Multipla) research fellowship to EC code n. 2019/BS/015 and financed or co-financed with the '5 per mille' public funding; and by Wellcome Trust, the BBSRC and Parkinson's UK to AJG. We thank Dr. Federica Cherchi for helping with the Graphical Abstract.

Author contribution. EC conceived the project and performed the experiments, EC and AJG analyzed the data and wrote the manuscript.

Conflicts of Interest. The authors declare no conflict of interest.

Declaration of transparency and scientific rigour.
This Declaration acknowledges that this paper adheres to the principles for transparent reporting and scientific rigour of preclinical research as stated in the BJP guidelines for Design & Analysis and Animal Experimentation, and as recommended by funding agencies, publishers and other organizations engaged with supporting research.

Data availability statement.
The data that support the findings of this study are available from the corresponding author upon reasonable request.

References

Albers, G. W., Goldberg, M. P., & Choi, D. W. (1989). N-Methyl-D-Aspartate antagonists - Ready for clinical-trial in brain ischemia. *Annals of Neurology, 25*(4), 398-403. doi:10.1002/ana.410250412

Alexander, S. P. H, Kelly, E., Mathie, A., Peters, J. A., Veale, E. L., Armstrong, J. F., Faccenda, E., Harding, S. D., Pawson, A. J., Southan, C., Buneman, O. P., Cidlowski, J. A., Christopoulos, A., Davenport, A. P., & Collaborators. The Concise Guide to PHARMACOLOGY 2021/22: Introduction and Other Protein Targets.British Journal of Pharmacology(2021) 178, S1-S26. e: http://onlinelibrary.wiley.com/doi/10.1111/bph.15537/full

Allen, N. J., Rossi, D. J., & Attwell, D. (2004). Sequential release of GABA by exocytosis and reversed uptake leads to neuronal swelling in simulated ischemia of hippocampal slices. *Journal of Neuroscience, 24*(15), 3837-3849. doi:10.1523/jneurosci.5539-03.2004

Antonioli, L., Blandizzi, C., Pacher, P., & Haskó, G. (2013). Immunity, inflammation and cancer: a leading role for adenosine. *Nature Review Cancer 13*(12):842-57. doi: 10.1038/nrc3613.

Arcangeli, S., Tozzi, A., Tantucci, M., Spaccatini, C., de Iure, A., Costa, C., … Calabresi, P. (2013). Ischemic-LTP in striatal spiny neurons of both direct and indirect pathway requires the activation of D1-like receptors and NO/soluble guanylate cyclase/cGMP transmission. *Journal of Cerebral Blood Flow and Metabolism, 33*(2), 278-286. doi:10.1038/jcbfm.2012.167

Blank Jr, W.F. & Kirshner, H.S. (1977). The kinetics of extracellular potassium changes during hypoxia and anoxia in the cat cerebral cortex. *Brain Research*. 123(1):113-24. doi: 10.1016/0006-8993(77)90646-1.

Cao, J. Y., Dorris, D. M., & Meitzen, J. (2018). Electrophysiological properties of medium spiny neurons in the nucleus accumbens core of prepubertal male and female Drd1a-tdTomato line 6 BAC transgenic mice. *Journal of Neurophysiology, 120*(4), 1712-1727. doi:10.1152/jn.00257.2018

Choi, D. W., & Rothman, S. M. (1990). The role of glutamate neurotoxicity in hypoxic-ischemic neuronal death. *Annual Review of Neuroscience, 13*, 171-182. doi:10.1146/annurev.neuro.13.1.171

Coppi, E., Pedata, F., & Gibb, A. J. (2012). P2Y(1) receptor modulation of Ca2+-activated K+ currents in medium-sized neurons from neonatal rat striatal slices. *Journal of Neurophysiology, 107*(3), 1009-1021. doi:10.1152/jn.00816.2009

Coppi, E., Cellai, L., Maraula, G., Pugliese, A. M., & Pedata, F. (2013). Adenosine A2A receptors inhibit delayed rectifier potassium currents and cell differentiation in primary purified oligodendrocyte cultures. Neuropharmacology 73:301-10. https://doi.org/10.1016/j.neuropharm.2013.05.035.

Cunha, R. A., Constantino, M. D., & Ribeiro, J. A. (1999). G Protein coupling of CGS 21680 binding sites in the rat hippocampus and cortex is different from that of adenosine A(1) and striatal A(2A) receptors. *Naunyn-Schmiedebergs Archives of Pharmacology, 359*(4), 295-302. doi:10.1007/pl00005355

Curtis, M. J., Alexander, S., Cirino, G., Docherty, J. R., George, C. H., Giembycz, M. A., … Ahluwalia, A. (2018). Experimental design and analysis and their reporting II: updated and simplified guidance for authors and peer reviewers. *British Journal of Pharmacology, 175*(7), 987-993. doi:10.1111/bph.14153

Dettori, I., Gaviano, L., Ugolini, F., Lana, D., Bulli, I., Magni, G., … Pedata, F. (2021). Protective Effect of Adenosine A(2B) Receptor Agonist, BAY60-6583, Against Transient Focal Brain Ischemia in Rat. *Frontiers in Pharmacology, 11*doi:10.3389/fphar.2020.588757

Dias, R. B., Ribeiro, J. A., & Sebastiao, A. M. (2012). Enhancement of AMPA currents and GluR1 membrane expression through PKA-coupled adenosine A2A receptors. *Hippocampus, 22*(2), 276-291. doi:10.1002/hipo.20894

Duffy, S. M., Cruse, G., Brightling, C. E., & Bradding, P. (2007). Adenosine closes the K+ channel KCa3.1 in human lung mast cells and inhibits their migration via the adenosine A2A receptor. European Journal of Immunology 37(6):1653-62. https://doi.org/10.1002/eji.200637024.

Dunwiddie, T. V., & Diao, L. H. (1994). Extracellular adenosine concentrations in hippocampal brain-slices and the tonic inhibitory modulation of evoked excitatory responses. *Journal of Pharmacology and Experimental Therapeutics, 268*(2), 537-545.

Erecinska, M., & Silver, I. A. (1994). Ions and energy in mammalian brain. *Progress in Neurobiology, 43*(1), 37-71. doi:10.1016/0301-0082(94)90015-9

Fredholm, B. B., Ijzerman, A. P., Jacobson, K. A., Linden, J., & Muller, C. E. (2011). International Union of Basic and Clinical Pharmacology. LXXXI. Nomenclature and Classification of Adenosine Receptors-An Update. *Pharmacological Reviews, 63*(1), 1-34. doi:10.1124/pr.110.003285

Fusco, I., Ugolini, F., Lana, D., Coppi, E., Dettori, I., Gaviano, L., … Pugliese, A. M. (2018). The Selective Antagonism of Adenosine A(2B) Receptors Reduces the Synaptic Failure and Neuronal Death Induced by Oxygen and Glucose Deprivation in Rat CA1 Hippocampus in Vitro. *Frontiers in Pharmacology, 9*doi:10.3389/fphar.2018.00399

Fusco, I., Cherchi, F., Catarzi, D., Colotta, V., Pedata, F., Pugliese, A. M., & Coppi, E. (2019). Functional characterization of a novel adenosine A2B receptor agonist on short-term plasticity and synaptic inhibition during oxygen and glucose deprivation in the rat CA1 hippocampus. *Brain Res Bulletin 151*:174-180. doi: 10.1016/j.brainresbull.2019.05.018

Goncalves, F. Q., Pires, J., Pliassova, A., Beleza, R., Lemos, C., Marques, J. M., … Rial, D. (2015). Adenosine A(2b) receptors control A(1) receptor-mediated inhibition of synaptic transmission in the mouse hippocampus. *European Journal of Neuroscience, 41*(7), 876-886. doi:10.1111/ejn.12851

Guatteo, E., Federici, M., Siniscalchi, A., Knopfel, T., Mercuri, N. B., & Bernardi, G. (1998). Whole cell patch-clamp recordings of rat midbrain dopaminergic neurons isolate a sulphonylurea- and ATP-sensitive component of potassium currents activated by hypoxia. *Journal of Neurophysiology, 79*(3), 1239-1245.

Gui, L., Duan, W., Tian, H., Li, C., Zhu, J., Chen, J. F., & Zheng, J. (2009). Adenosine A2A receptor deficiency reduces striatal glutamate outflow and attenuates brain injury induced by transient focal cerebral ischemia in mice. Brain Research 1297:185-93. https://doi.org/10.1016/j.brainres.2009.08.050.

Hansen, A. J. (1985). Effect of anoxia on ion distribution in the braiN. *Physiological Reviews, 65*(1), 101-148.

Heurteaux, C., Bertaina, V., Widmann, C., & Lazdunski, M. (1993). K+ channel openers prevent global ischemia-induced expression of c-fos, c-jun, heat shock protein, and amyloid beta-protein precursor genes and neuronal death in rat hippocampus. Proceedings of the National Academy of Sciences US 90(20):9431-5. https://doi.org/10.1073/pnas.90.20.9431.

Hibino, H., Inanobe, A., Furutani, K., Murakami, S., Findlay, I., & Kurachi, Y. (2010). Inwardly Rectifying Potassium Channels: Their Structure, Function, and Physiological Roles. *Physiological Reviews, 90*(1), 291-366. doi:10.1152/physrev.00021.2009

Ikonomidou, C., & Turski, L. (2002). Why did NMDA receptor antagonists fail clinical trials for stroke and traumatic brain injury? *Lancet Neurology, 1*(6), 383-386. doi:10.1016/s1474-4422(02)00164-3

Jarvis, C. R., Anderson, T. R., & Andrew, R. D. (2001). Anoxic depolarization mediates acute damage independent of glutamate in neocortical brain slices. *Cerebral Cortex, 11*(3), 249-259. doi:10.1093/cercor/11.3.249

Karunasinghe, R. N., & Lipski, J. (2013). Oxygen and glucose deprivation (OGD)-induced spreading depression in the Substantia Nigra. *Brain Research, 1527*, 209-221. doi:10.1016/j.brainres.2013.06.016

Latini, S., Bordoni, F., Pedata, F., & Corradetti, R. (1999). Extracellular adenosine concentrations during in vitro ischaemia in rat hippocampal slices. *British Journal of Pharmacology, 127*(3), 729-739. doi:10.1038/sj.bjp.0702591

Le Moine, C., Svenningsson, P., Fredholm, B. B., & Bloch, B. (1997). Dopamine-adenosine interactions in the striatum and the globus pallidus: inhibition of striatopallidal neurons through either D2 or A2A receptors enhances D1 receptor-mediated effects on c-fos expression. Journal of Neuroscience 17(20):8038-48. https://doi.org/10.1523/JNEUROSCI.17-20-08038.1997.

Li, Q., Han, X. N., Lan, X., Hong, X. H., Gao, Y. F., Luo, T. Q., … Wang, J. (2017). Inhibition of tPA-induced hemorrhagic transformation involves adenosine A2b receptor activation after cerebral ischemia. *Neurobiology of Disease, 108*, 173-182. doi:10.1016/j.nbd.2017.08.011

Lilley, E., Stanford, S. C., Kendall, D. E., Alexander, S. P., Cirino, G., Docherty, J. R., George, C. H., Insel, P. A., Izzo, A. A., Ji, Y., Panettieri, R. A., Sobey, C. G., Stefanska, B., Stephens, G., Teixeira, M., & Ahluwalia, A. (2020). ARRIVE 2.0 and the British Journal of Pharmacology: Updated guidance for 2020. British Journal of Pharmacology, 177(16), 3611–3616. .

Lloyd, H. G. E., & Fredholm, B. B. (1995). Involvement of adenosine-deaminase and adenosine kinase in regulating extracellular adenosine concentration in rat hippocampal slices. *Neurochemistry International, 26*(4), 387-395. doi:10.1016/0197-0186(94)00144-j

Lopes, L. V., Cunha, R. A., Kull, B., Fredholm, B. B., & Ribeiro, J. A. (2002). Adenosine A(2A) receptor facilitation of hippocampal synaptic transmission is dependent on tonic A(1) receptor inhibition. *Neuroscience, 112*(2), 319-329. doi:10.1016/s0306-4522(02)00080-5

Madl, J. E., & Burgesser, K. (1993). Adenosine-triphosphate depletion reverses sodium-dependent, neuronal uptake of glutamate in rat hippocampal slices. *Journal of Neuroscience, 13*(10), 4429-4444.

Maraula, G., Traini, C., Mello, T., Coppi, E., Galli, A., Pedata, F., & Pugliese, A. M. (2013). Effects of oxygen and glucose deprivation on synaptic transmission in rat dentate gyrus:.Role of A(2A) adenosine receptors. *Neuropharmacology, 67*, 511-520. doi:10.1016/j.neuropharm.2012.12.002

Matucz, E., Moricz, K., Gigler, G., Benedek, A., Barkoczy, J., Levay, G., … Szenasi, G. (2006). Therapeutic time window of neuroprotection by non-competitive AMPA antagonists in transient and permanent focal cerebral ischemia in rats. *Brain Research, 1123*, 60-67. doi:10.1016/j.brainres.2006.09.043

Melani, A., Corti, F., Cellai, L., Vannucchi, M. G., & Pedata, F. (2014). Low doses of the selective adenosine A(2A) receptor agonist CGS21680 are protective in a rat model of transient cerebral ischemia. *Brain Research, 1551*, 59-72. doi:10.1016/j.brainres.2014.01.014

Melani, A., Dettori, I., Corti, F., Cellai, L., & Pedata, F. (2015). Time-course of protection by the selective A(2A) receptor antagonist SCH58261 after transient focal cerebral ischemia. *Neurological Sciences, 36*(8), 1441-1448. doi:10.1007/s10072-015-2160-y

Melani, A., Pantoni, L., Bordoni, F., Gianfriddo, M., Bianchi, L., Vannucchi, M. G., … Pedata, F. (2003). The selective A(2A) receptor antagonist SCH 58261 reduces striatal transmitter outflow, turning behavior and ischemic brain damage induced by permanent focal ischemia in the rat. *Brain Research, 959*(2), 243-250. doi:10.1016/s0006-8993(02)03753-8

Nakajima, M., Suda, S., Sowa, K., Sakamoto, Y., Nito, C., Nishiyama, Y., … Kimura, K. (2018). AMPA Receptor Antagonist Perampanel Ameliorates Post-stroke Functional and Cognitive Impairments. *Neuroscience, 386*, 256-264. doi:10.1016/j.neuroscience.2018.06.043

Obeidat, A. S., & Andrew, R. D. (1998). Spreading depression determines acute cellular damage in the hippocampal slice during oxygen/glucose deprivation. *European Journal of Neuroscience, 10*(11), 3451-3461. doi:10.1046/j.1460-9568.1998.00358.x

Oliet, S. H., & Poulain, D. A. (1999). Adenosine-induced presynaptic inhibition of IPSCs and EPSCs in rat hypothalamic supraoptic nucleus neurons. Journal of Physiology 1;520 Pt 3(Pt 3):815-25. https://doi.org/10.1111/j.1469-7793.1999.00815.x.Ortega-Gutierrez, S., Jones, B., Mendez-Ruiz, A., Shah, P., & Torbey, M. T. (2020). Adenosine Receptor Modulation of Hypoxic-ischemic Injury in Striatum of Newborn Piglets. *Current Neurovascular Research, 17*(4), 510-517. doi:10.2174/1567202617999200831152233

Pedata, F., Dettori, I., Coppi, E., Melani, A., Fusco, I., Corradetti, R., & Pugliese, A. M. (2016). Purinergic signalling in brain ischemia. *Neuropharmacology, 104*, 105-130. doi:10.1016/j.neuropharm.2015.11.007

Percie du Sert, N., Hurst, V., Ahluwalia, A., Alam, S., Avey, M. T., Baker, M., Browne, W. J., Clark, A., Cuthill, I. C., Dirnagl, U., Emerson, M., Garner, P., Holgate, S. T., Howells, D. W., Karp, N. A., Lazic, S. E., Lidster, K., MacCallum, C. J., Macleod, M., … Würbel, H. (2020). The ARRIVE guidelines 2.0: Updated guidelines for reporting animal research. PLoS Biology, 18(7), e3000410. https://doi.org/10.1371/journal.pbio.3000410

Pugliese, A. M., Coppi, E., Spalluto, G., Corradetti, R., & Pedata, F. (2006). A(3) adenosine receptor antagonists delay irreversible synaptic failure caused by oxygen and glucose deprivation in the rat CA1 hippocampus in vitro. *British Journal of Pharmacology, 147*(5), 524-532. doi:10.1038/sj.bjp.0706646

Pugliese, A. M., Coppi, E., Volpini, R., Cristalli, G., Corradetti, R., Jeong, L. S., … Pedata, F. (2007). Role of adenosine A(3) receptors on CA1 hippocampal neurotransmission during oxygen-glucose deprivation episodes of different duration. *Biochemical Pharmacology, 74*(5), 768-779. doi:10.1016/j.bcp.2007.06.003

Rosen, A. S., & Morris, M.E. (1994). Influence of temperature on anoxic responses of neocortical pyramidal neurons. Neuroscience 63(4):949-55. https://doi.org/10.1016/0306-4522(94)90563-0.

Rossi, D. J., Oshima, T., & Attwell, D. (2000). Glutamate release in severe brain ischaemia is mainly by reversed uptake. *Nature, 403*(6767), 316-321. doi:10.1038/35002090

Rymar, V. V., Sasseville, R., Luk, K. C., & Sadikot, A. F. (2004). Neurogenesis and stereological morphometry of calretinin-immunoreactive GABAergic interneurons of the neostriatum. *Journal of Comparative Neurology, 469*(3), 325-339. doi:10.1002/cne.11008

Saegusa, N., Sato, T., Ogura, T., Komuro, I., & Nakaya, H. (2004). Inhibitory effects of AMP 579, a novel cardioprotective adenosine A1/A2A receptor agonist, on native IKr and cloned HERG current. Naunyn-Schmiedeberg's Archives of Pharmacology 370(6):492-9. https://doi.org/10.1007/s00210-004-0999-1.

Stone, T. W. (2005). Adenosine, neurodegeneration and neuroprotection. *Neurological Research, 27*(2), 161-168. doi:10.1179/016164105x21896

Szatkowski, M., Barbour, B., & Attwell, D. (1990). Non-vesicular release of glutamate from glial-cells by reversed electrogenic glutamate uptake. *Nature, 348*(6300), 443-446. doi:10.1038/348443a0.

Tambasco, N., Romoli, M., & Calabresi, P. (2018). Selective basal ganglia vulnerability to energy deprivation: Experimental and clinical evidences. Progress in Neurobiology 169:55-75. https://doi.org/10.1016/j.pneurobio.2018.07.003

Ueda, Y., Obrenovitch, T. P., Lok, S. Y., Sarna, G. S., & Symon, L. (1992). Changes in extracellular glutamate concentration produced in the rat striatum by repeated ischemia. Stroke 23(8):1125-30. https://doi.org/10.1161/01.str.23.8.1125.

Vigil, F.A., Bozdemir, E., Bugay, V., Chun, S.H., Hobbs, M., Sanchez, I., Hastings, S.D., Veraza, R. J., Holstein, D. M., Sprague, S. M., M. Carver, C., Cavazos, J. E., Brenner, R., Lechleiter, J. D., & Shapiro, M. S. (2020). Prevention of brain damage after traumatic brain injury by pharmacological enhancement of KCNQ (Kv7, "M-type") K(+) currents in neurons. Journal of Cerebral Blood Flow & Metabolism 40(6):1256-1273. https://doi.org/10.1177/0271678X19857818

von Lubitz, D., Ye, W., McClellan, J., & Lin, R. C. S. (1999). Stimulation of adenosine A(3) receptors in cerebral ischemia - Neuronal death, recovery, or both? *Neuroprotective Agents: Fourth International Conference, 890*, 93-106.

Wahl, F., Obrenovitch, T. P., Hardy, A. M., Plotkine, M., Boulu, R., & Symon, L. (1994). Extracellular glutamate during focal cerebral-ischemia in rats - Time-course and calcium dependency. *Journal of Neurochemistry, 63*(3), 1003-1011.

Wu, N., Cepeda, C., Zhuang, X., & Levine, M. S. (2007). Altered corticostriatal neurotransmission and modulation in dopamine transporter knock-down mice. Journal of Neurophysiology 98(1):423-32. https://doi.org/10.1152/jn.00971.2006.

Zocchi, C., Ongini, E., Conti, A., Monopoli, A., Negretti, A., Baraldi, P. G., & Dionisotti, S. (1996). The non-xanthine heterocyclic compound SCH 58261 is a new potent and selective A(2a) adenosine receptor antagonist. *Journal of Pharmacology and Experimental Therapeutics, 276*(2), 398-404.

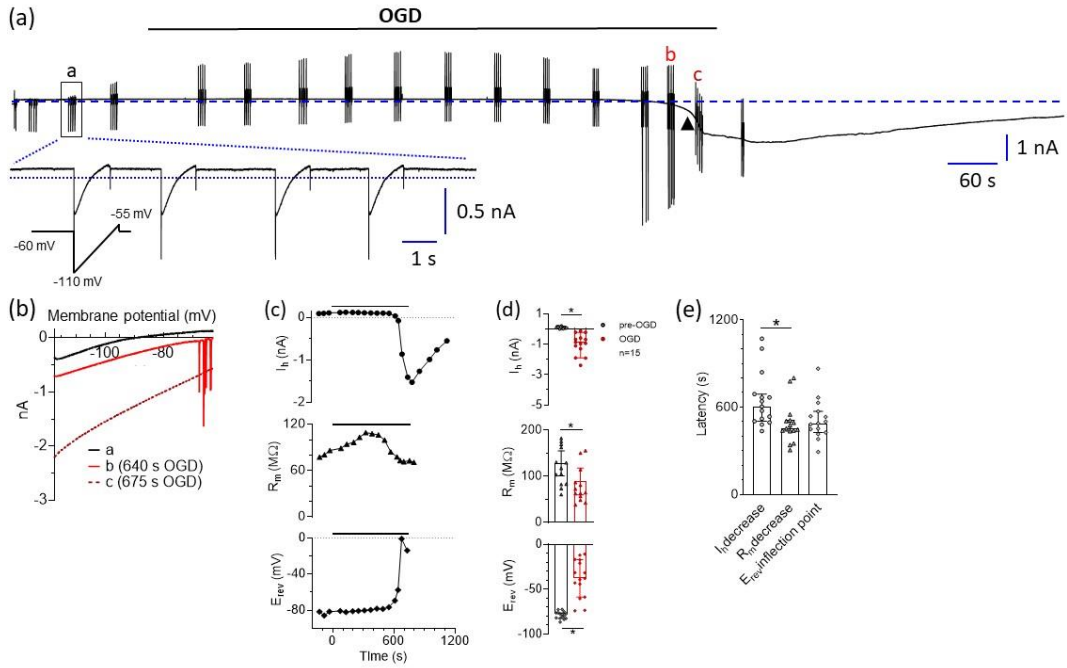

Figure 1: A prolonged oxygen and glucose deprivation (OGD) insult in striatal medium spiny neurons triggers a series of electrophysiological changes which ultimately lead to the appearance of anoxic depolarization (AD). (a) Representative whole-cell patch-clamp trace recorded at -60 mV from a medium spiny neuron (MSN) in a P28 rat striatal slice subjected to OGD conditions. OGD was applied until the sudden increase in holding current (I_h) reached a steady state level (arrowhead: at 710 s in this representative cell). *Lower inset*: expanded time scale of the 4 voltage ramp traces (from -113 to -63 mV, duration 1 s; 2 s inter-episode interval) in "a" is shown an example of the measurement of the membrane resistance (R_m) and the current reversal potential (E_{rev}). A trial consisting of 4 ramps was applied in each recorded cell every 60 s. **(b)** Current-Voltage (I-V) relationship of ramp traces recorded in the same cell at different time points: before OGD (trial a), during OGD but immediately before anoxic depolarization (AD: trial in b) and during AD (trial in c). Each ramp is the average of 4 individual voltage traces within each trial examined. **(c)** Time course of changes in I_h (*upper panel*), R_m (*middle panel*) and E_{rev} (*lower panel*) in the same cell. **(d)** Pooled data (median ± 95% confidence interval: CI) of I_h (*upper panel*), R_m (*middle panel*) and E_{rev} (*lower panel*) measured in 15 cells before (pre-OGD: last 2 min before OGD) or during OGD (last 2 min of OGD). * $P < 0.05$; Wilcoxon test. **(e)** Pooled data of the latency (measured from OGD start) to reach I_h increase > 20% (circles), R_m decrease > 20% (triangles) or E_{rev} inflection point (diamonds) in 21 cells recorded. * $P < 0.05$; Dunn's multiple comparisons test.

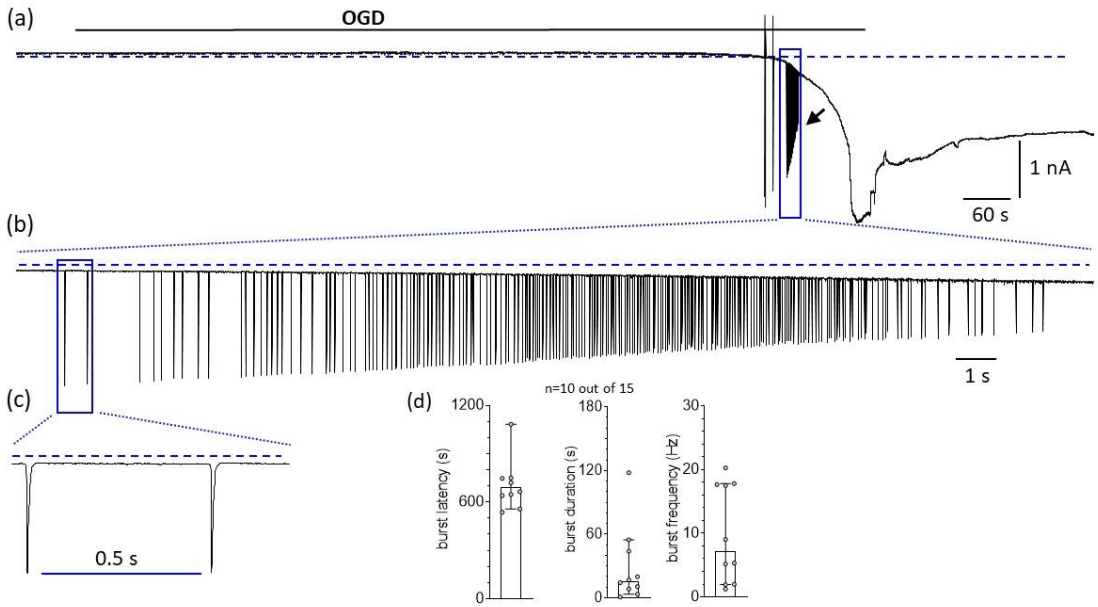

Figure 2: In a subset of striatal medium spiny neurons, OGD induced a burst of repetitive action potentials during anoxic depolarization (AD). (a) Original patch-clamp current trace recorded in a -60 mV clamped medium spiny neuron (MSN) from a p28 rat striatal slice where an oxygen and glucose deprivation (OGD) insult was applied. In this particular cell no voltage ramps were elicited. OGD was prolonged until the increase of holding current (I_h) reached a steady state level (980 s in this particular MSN). Arrow indicates the burst of spontaneous action potentials (APs) that accompanies the AD phase. **(b,c)** Progressively expanded time scales of the same event. **(d)** Pooled data (median ± 95% confidence interval: CI) of burst latency (*left panel*), duration (*central panel*) or frequency (*right panel*) in 10 out of 15 slices in which the spontaneous burst was recorded.

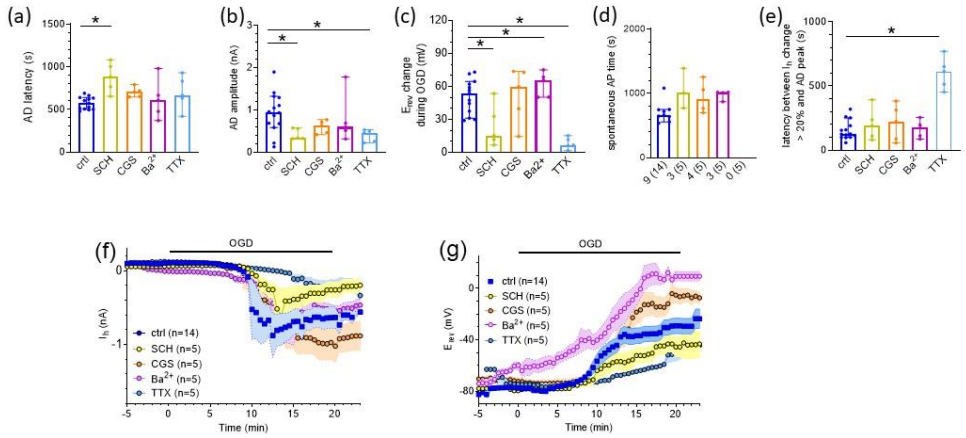

Figure 3: The $A_{2A}R$ antagonist SCH58261 delayed the appearance of anoxic depolarization (AD) induced by OGD in rat striatal medium spiny neurons. (a-e). Pooled data (median ± 95% confidence interval: CI) of AD latency (measured as the time needed for I_h to change more that 20% from OGD start: **a**), AD amplitude (measured as the difference between pre-OGD I_h value and the AD peak: **b**), E_{rev} changes during OGD (measured as the difference between pre-OGD E_{rev} value and the value reached during the AD peak: **c**), the latency to initiate the spontaneous action potential (AP) burst (when detected) (**d**) and the latency between I_h change (more than 20%) and AD peak (**e**) in striatal medium spiny neurons (MSNs) in different experimental conditions: untreated OGD slices (ctrl; blue circles) or slices subjected to OGD in the presence of different pharmacological treatments: the $A_{2A}R$ antagonist SCH58261 (SCH, 10 µM; yellow circles); the $A_{2A}R$ agonist CGS21680 (CGS, 1 µM; orange circles); the K^+ channel blocker Ba^{2+} (2 mM; purple circles) or Na^+ channel blocker tetrodotoxin (TTX, 1 µM; green circles). Each compound was added at least 10 min before OGD and throughout the insult. Note that the proportion of MSNs presenting the burst of APs during OGD is reported below each column in **(d)**. **(f,g).** Averaged time courses of of I_h (**e**) or E_{rev} (**f**) before or during OGD performed in different experimental groups. * $P < 0.05$; Dunn's multiple comparisons test.

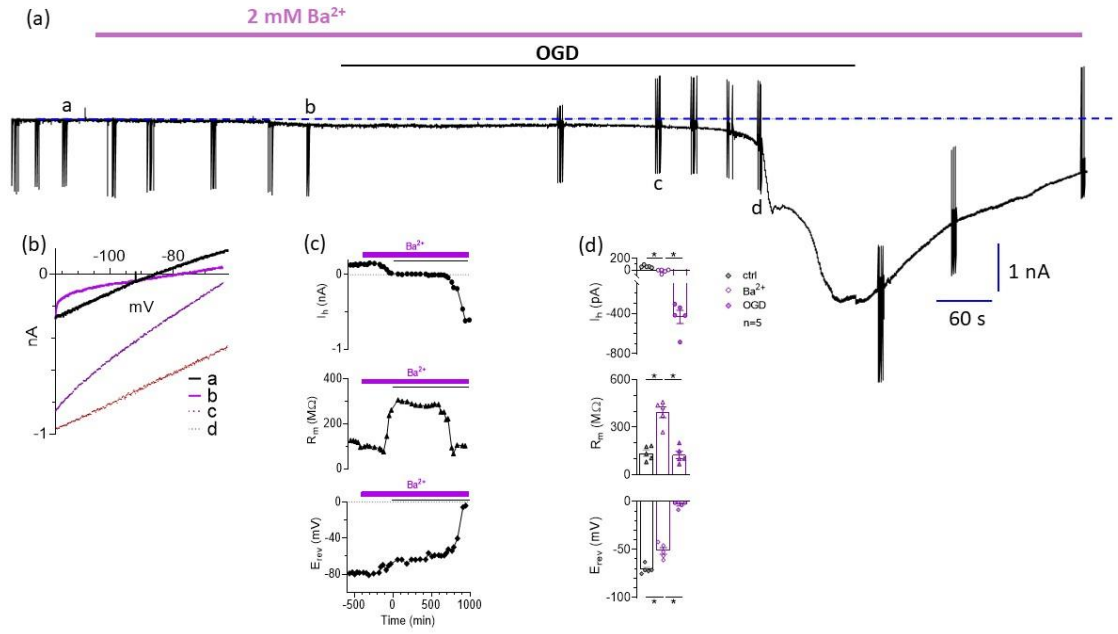

Figure 4: Ba^{2+}-induced electrophysiological changes before or during oxygen and glucose deprivation (OGD) in striatal medium spiny neurons. (a) Original patch-clamp current trace recorded in a -60 mV clamped medium spiny neuron (MSN) from a p28 rat striatal slice where an OGD insult was applied in the presence of extracellular Ba^{2+} (2 mM). OGD was prolonged until the increase in holding current (I_h) reached a steady state level (760 s in this particular MSN). Downward deflections are ramp protocols (from -113 to -63 mV in 1 s, 2 s inter-episode interval) evoked to measure the membrane current reversal potential (E_{rev}) and membrane resistance (R_m) at different time points. A trial consisting of four consecutive ramp episodes was repeated every 60 s. **(b)** Current-to-Voltage (I-V) relationship of ramp traces recorded in the same cell at different time points: before the application of Ba^{2+} (trial a), after 5 minutes of Ba^{2+} application and before OGD (trial b), during OGD but immediately before anoxic depolarization (AD: trial in c) and during AD (trial in c). Each ramp is the average of 4 individual voltage traces within each trial examined. **(c)** Time courses of I_h (*upper panel*), R_m (*middle panel*) and E_{rev} (*lower panel*) recorded in the same representative cell. **(d)** Pooled data (mean ± SEM) of I_h (*upper panel*), R_m (*middle panel*) and E_{rev} (*lower panel*) changes measured in control conditions (ctrl: grey symbols), in Ba^{2+} (open purple symbols: last 2 min before OGD in Ba^{2+}) or during OGD in Ba^{2+} (filled purple symbols: last 2 min of OGD in Ba^{2+}). * $P < 0.05$, paired Student's *t*-test.

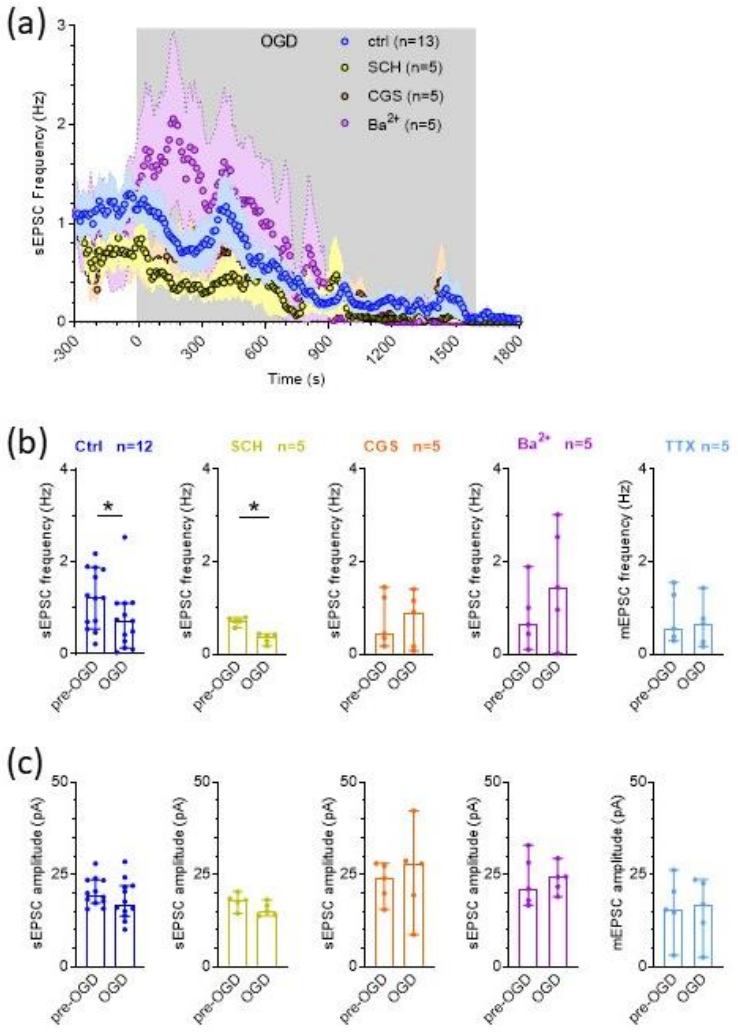

Figure 5: Oxygen and glucose deprivation (OGD) caused a decrease in the frequency of spontaneous, but not miniature, excitatory post-synaptic currents (EPSCs) in medium spiny neurons, an effect prevented by K^+ channel block and by the selective stimulation of A_{2A}Rs. (a) Averaged time courses of spontaneous or miniature EPSCs (sEPSCs or mEPSCs, respectively) event frequency recorded in MSNs subjected to OGD in different experimental conditions: in control conditions (ctrl: blue circles; n=12); in the presence of the A_{2A}R antagonist SCH58261 (SCH, 10 µM: yellow circles; n=5); in the presence of the A_{2A}R agonist CGS21680 (CGS, 1 µM: orange circles; n=5); in Ba^{2+} (2 mM: purple circles; n=5) or in tetrodotoxin (TTX, 1 µM: green circles; n=5). **(b,c)** Pooled data (median ± 95% confidence interval: CI) of event frequency (**b**) or amplitude (**c**) measured during the last 2 min before OGD (pre-OGD) or between 3 and 5 min OGD (OGD) in different experimental groups. * *P* <0.05; Wilcoxon test.

Graphical Abstract